Investigation of D(d,n)He^3 Neutrons at 8.4 Mev*

W. W. DAEHNICK AND J. M. FOWLER
Wayman Crow Laboratory of Physics, Washington University, St. Louis, Missouri

(Received May 15, 1958)

The angular distribution of neutrons from the reaction D(d,n)He^3 has been obtained at 8.4±0.1 Mev incident deuteron energy for center-of-mass angles 2° to 84°. A single plastic crystal was used as a detector and deuterium gas at 200 psi as a target. The distribution is fitted by a sum of Legendre polynomials. It is also compared with the predictions of nuclear stripping theory, and adequate agreement is found with an angular distribution of the form $d\sigma/d\Omega \propto h_d^2 - \frac{2}{3}h_d h_{d'} + h_{d'}^2$, where the h_d and $h_{d'}$ represent the simple Butler stripping distributions for the incident and target deuterons, respectively. The interaction radius necessary was $R_0 = 7\times10^{-13}$ cm.

I. INTRODUCTION

THE D(d,n)He^3 reaction has been the subject of many investigations both experimental and theoretical. (A thorough list of references is given in a recent article by Fowler and Brolley.[1]) It is of importance experimentally, as a source of fast neutrons, and theoretically, because it is one of the less complex nucleus-nucleus reactions.

The early work of Konopinski *et al.*[2] showed that by considering the centrifugal barriers for different deuteron partial waves, one should be able to fit the observed angular distributions with a sum of Legendre polynomials. An exact calculation of these coefficients over an extended energy range has not been attempted; the usual technique is to use them as adjustable parameters, and since at deuteron energies in the neighborhood of 10-Mev polynomials to order ten are needed (even polynomials only), one has six adjustable parameters with which to approximate the observed angular distribution and quite adequate fits are obtained.

Other authors, notably Fairbairn[3] and Chagnon and Owen,[4] have utilized the approach of stripping theory. Fairbairn used the same stripping approach as Butler[5] but appropriately symmetrized his wave functions to take into account the identity of the incident and target particles. His predicted distribution was compared to observed high-energy data, ~20-Mev deuterons, and was in qualitative agreement at the forward angles. Chagnon and Owen obtained the angular distributions for deuterons of energy ranging from 250 kev to 825 kev and found that a Born approximation approach, properly symmetrized, would fit the data over that energy range if the interaction radius was allowed to decrease slowly with energy, from 8.2×10^{-13} cm to 7.15×10^{-13} cm.

Brolley, Putman, and Rosen[6] recently reported an experimental investigation of the D+d reaction covering a range of deuteron energies from 8 to 14 Mev. In the D(d,n)He^3 reaction, using emulsion techniques, they detected the He^3 particle rather than the neutron and thus the angular range they were able to cover was limited to center-of-mass angles greater then 30°. As the forward neutron angles are of great interest if one wishes to compare the data with stripping theory, an experiment in which the neutrons were detected directly was undertaken.

II. EXPERIMENTAL TECHNIQUE

A. Apparatus

In Fig. 1 a schematic view of the experiment is given. A beam of fast deuterons strikes a D_2 target of 600 kev thickness. The deuterium gas target consists of a thin-walled cylindrical chamber of 1-inch diameter with 0.001-inch stainless steel entrance and exit foils, which is filled with D_2 gas at 200 psi 10-Mev deuterons from the Washington University cyclotron, after passing through the monitor foil, the vacuum exit foil, target entrance foil, and half the gas target, have a residual energy of 8.4±0.1 Mev. The beam leaves the target through the exit window and stops in air.

The neutrons are detected directly by a plastic scintillation crystal (Nuclear Enterprises Ltd. Ne 102), and the pulse-height spectrum is analyzed and displayed

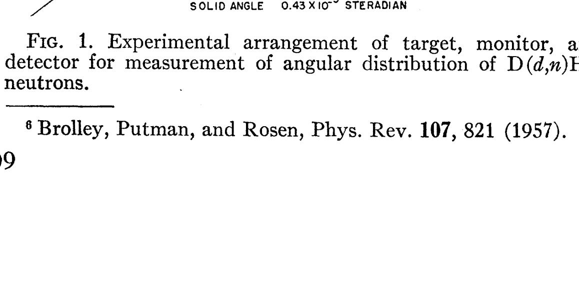

FIG. 1. Experimental arrangement of target, monitor, and detector for measurement of angular distribution of D(d,n)He^3 neutrons.

* Supported in part by the U. S. Air Force through the Office of Scientific Research of the Air Force Research and Development Command.

[1] J. L. Fowler and J. E. Brolley, Jr., Revs. Modern Phys. **28**, 103 (1956).
[2] Beiduk, Pruett, and Konopinski, Phys. Rev. **77**, 622 (1950).
[3] W. M. Fairbairn, Proc. Phys. Soc. (London) **A67**, 990 (1954).
[4] P. R. Chagnon and G. E. Owen, Phys. Rev. **101**, 1798 (1956).
[5] S. T. Butler, Proc. Roy. Soc. (London) **A202**, 559 (1951).
[6] Brolley, Putman, and Rosen, Phys. Rev. **107**, 821 (1957).

by a 60-channel pulse-height analyzer of the Hutchinson-Scarrott type. The scintillation crystal ($1\times1\times0.25$ inch) is mounted in an iron shield of 2-inch wall thickness.

Since it was desired to measure the absolute cross sections for the reaction, accurate monitoring of the beam was necessary. After some experimentation, it was found quite satisfactory to scatter a small fraction of the collimated and focused beam into a small KI crystal by a thin (2.5 micron), Pt foil. Both total counts and counting rate were measured.

B. Procedure

In spite of careful shielding and target design, the background counting rate in unfavorable cases was often ten times as high as the neutron count. Thus each signal run was preceded and followed by a run with no D_2 in the target chamber in order to allow the accurate subtraction of background counts. Figures 2 and 3 show signal, background, and neutron spectra at a favorable and an unfavorable angle. The long dead time of the multichannel analyzer (500 microseconds average) made counting loss corrections necessary. The correction factor was found experimentally by counting the total number of pulses fed into the analyzer as well as those that were recorded. The unwanted detection of "breakup" neutrons was prevented by setting the analyzer bias at 4 Mev.

C. Errors

The method of subtracting the background spectra from the signal spectra proved quite satisfactory in all cases where the background did not greatly exceed the neutron counting rate. Background spectra taken under the same conditions but at different times were found to differ by as much as 2% due to changes in intensity and direction of the cyclotron beam during the runs. This time-dependent background caused a variation in counting rates, which caused gain shifts in the phototube (RCA 6199). Thus at large angles (90° c.m.), where about 90% of the total counting rate is background, a 1% uncertainty in the background spectrum will cause an 8% error in the neutron spectrum. At small angles, the same effect caused errors of only 0.4% because of the better signal to background ratio.

Other errors in the final results are due to the limited accuracy with which the crystal properties are known. An error of 2% is estimated for the determination of the absolute detection efficiency and uncertainties in the nonlinearity corrections of the plastic crystal used. Statistical errors of the neutron spectra range from 0.1% at 0° c.m. to 0.6% at 90° c.m. The error in the determination of the gas pressure of the target is about 1%. All geometrical uncertainties (solid angles, foil thicknesses, distances) should cause an absolute error not larger than 0.2%.

Thus the absolute probable errors range from 2.5% to 8.5% as indicated in Table I.

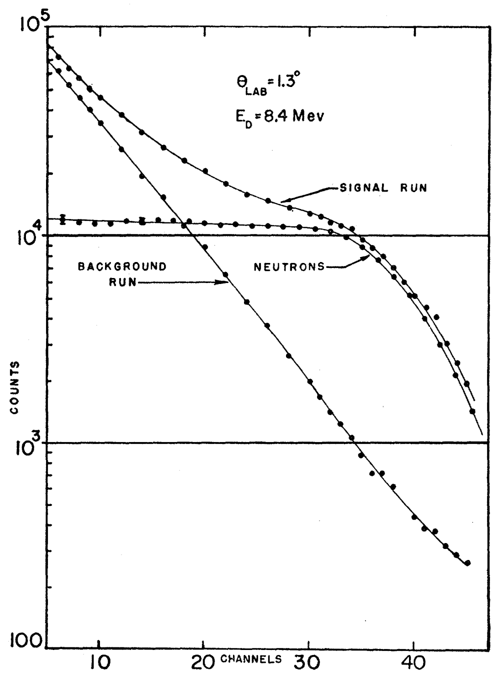

FIG. 2. Pulse-height spectrum of neutrons from $D(d,n)He^3$ at 1.3° lab. Background was taken with no D_2 in target chamber.

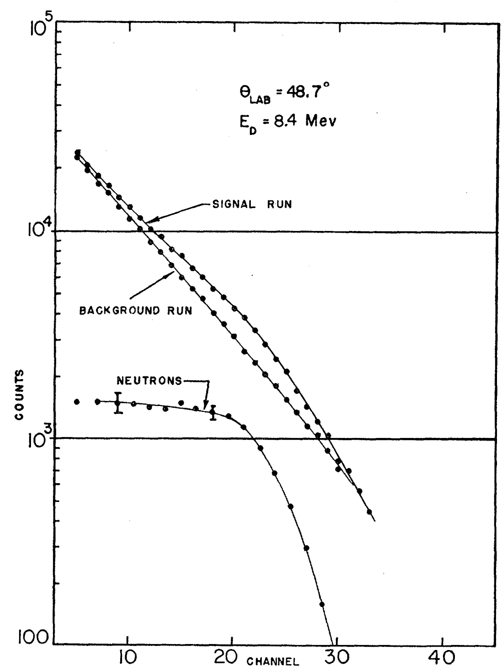

FIG. 3. Pulse-height spectrum of neutrons from $D(d,n)He^3$ at 48.7° lab. Background was taken with no D_2 in target chamber.

TABLE I. Angular dependance of the neutrons from D(d,n)He^3 at $E_d=8.4\pm0.1$ Mev. Angular resolution $<\pm1°$.

Neutron lab angle (deg)	$d\sigma/d\Omega$ (mb/steradian)	Absolute error (%)
1.3	89.6	±2.5
5.6	78.9	2.5
8.7	67.5	3
11.3	58.8	3
13.7	45.8	3
16.3	37.1	3.5
18.7	27.4	3.5
21.3	18.9	4
26.3	10.2	4.5
31.3	4.8	5
41.3	4.3	6
48.7	6.2	7
51.3	7.9	8
61.3	6.7	8.5

D. Data

The experimental $N(E)$ *vs* E curves were integrated and extrapolated to zero in order to obtain the total number of neutrons detected. The nonlinear pulse-height energy response of the plastic crystal for heavy particles was taken into account by using Birks' formula[7]

$$dP/dE=1/(1+kBdE/dx), \tag{1}$$

where kB is a constant that depends only on the particular type of crystal which is used. From the pulse-height to energy relations found in this experiment we calculated $kB=0.002$ mg/kev cm^2. The value 0.003 ± 0.001 mg/cm^2 was found in a different experiment especially designed to measure kB.[8] These values are smaller by a factor 6 than the kB value for stilbene reported earlier.[9] Table I shows the experimental data for the angular distribution and the probable absolute errors; Fig. 4 shows these data in the center-of-mass system. The solid curve on Fig. 4 is a summation of Legendre polynomials

$$d\sigma/d\Omega=\sum_{\nu=0}^{12} a_\nu P_\nu(\theta), \tag{2}$$

where the a_ν were taken from Brolley, Putnam, and Rosen.[6] The agreement is well within experimental errors.

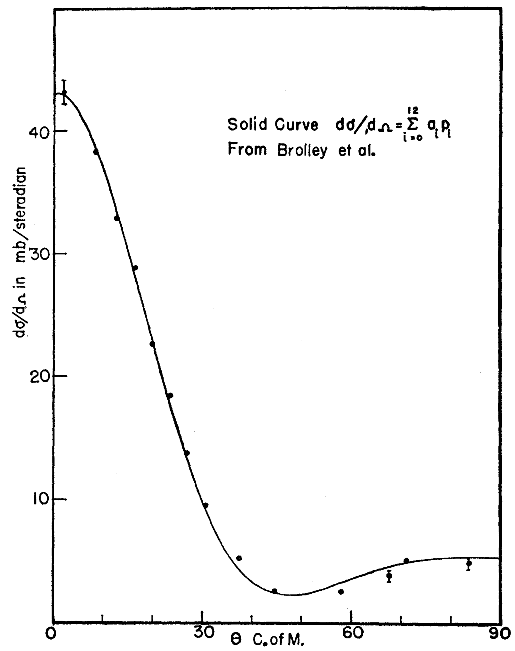

FIG. 4. Angular distribution of neutrons from D(d,n)He^3 at $E_d=8.4\pm0.1$ Mev fitted by sum of Legendre polynomials with coefficients from Brolley, Putman, and Rosen.[6]

III. DISCUSSION

The calculation of the differential cross section of D(d,n)He^3 using a stripping approach generally follows that of Owen and Madansky.[10] In the Born approximation the differential cross section is given by

$$d\sigma/d\Omega \propto \sum |\text{M.E.}|^2, \tag{3}$$

where $\sum$ indicates an average over initial and a sum over final spin orientation states. The matrix element is given by

$$\text{M.E.}=\int\cdots\int \psi_f{}^* U \psi_i, \tag{4}$$

with U the effective interaction potential among the nucleons involved and ψ_i, ψ_f the initial and final wave functions.

The initial wave function, appropriately symmetrized, will have the form

$$\psi_i=\psi_d(\mathbf{R}_n-\mathbf{R}_p)\psi_d(\mathbf{R}_{n'}-\mathbf{R}_{p'})\frac{1}{\sqrt{2}}\left\{\exp\left(i\mathbf{k}_d\cdot\frac{\mathbf{R}_n+\mathbf{R}_p}{2}\right)\exp\left(-i\mathbf{k}_d\cdot\frac{\mathbf{R}_{n'}+\mathbf{R}_{p'}}{2}\right)S_{dd'} +\exp\left(i\mathbf{k}_d\cdot\frac{\mathbf{R}_{n'}+\mathbf{R}_{p'}}{2}\right)\exp\left(-i\mathbf{k}_d\cdot\frac{\mathbf{R}_n+\mathbf{R}_p}{2}\right)S_{d'd}\right\}. \tag{5}$$

In Eq. (5) we have separated the internal motion and the center-of-mass motion, the primed quantities referring to the "target" deuteron and the unprimed to the "incident" deuteron. $S_{dd'}$ and $S_{d'd}$ are the appropriate combinations of deuteron spin wave functions for the initial total spin values of 2,1,0 (see for instance Schiff.[11]) If we further assume that the spin-orbit

[7] J. B. Birks, Proc. Phys. Soc. (London) **A64**, 874 (1951).
[8] R. Wilson (private communication).
[9] Swartz, Owen, and Ames, The Johns Hopkins University Report NYO-2053, 1957 (unpublished).
[10] G. E. Owen and L. Madansky, Phys. Rev. **105**, 1766 (1957).
[11] L. I. Schiff, Phys. Rev. **53**, 783 (1937).

term in the effective interaction potential is not important, so that the total *spin* angular momentum is conserved, we can immediately eliminate the initial state with total spin 2 from consideration; this follows since the protons in the final He^3 nucleus must be antiparallel so that the final total spin is at most 1.

In assembling the properly symmetrized final state wave function, our first requirement is that it be antisymmetric for exchange of the two neutrons as well as antisymmetric with respect to the two protons. If we treat the neutron space wave function as a plane wave and write the final state as a product of this with the internal He^3 space wave function γ_f, the complete final state wave function will have the form,

$$\psi_f=\frac{1}{\sqrt{2}}\bigg[\gamma_f(\mathbf{R}_{n'},\mathbf{R}_p,\mathbf{R}_{p'})e^{i\mathbf{k}_n\cdot\mathbf{R}_n}\times\exp\left(-i\mathbf{k}_n\cdot\frac{\mathbf{R}_{n'}+\mathbf{R}_{p'}+\mathbf{R}_p}{3}\right)\pm\gamma_f(\mathbf{R}_n,\mathbf{R}_p,\mathbf{R}_{p'})e^{i\mathbf{k}_n\cdot\mathbf{R}_{n'}}\times\exp\left(-i\mathbf{k}_n\cdot\frac{\mathbf{R}_n+\mathbf{R}_{p'}+\mathbf{R}_p}{3}\right)\bigg]\times S_{nn'}(\mp)S_{pp'}(-).\quad(6)$$

In Eq. (6), $\gamma_f(\mathbf{R}_{n\text{ or }n'},\mathbf{R}_{p'},\mathbf{R}_p)=\gamma_f(\mathbf{R}_{n'\text{ or }n},\mathbf{R}_p,\mathbf{R}_{p'})$, $(\pm)$ indicates the symmetric and the antisymmetric possibilities, and the primed and unprimed variables indicate, as before, quantities in the "target" and "incident" deuteron. The spin wave function for the protons in the He^3 nucleus, $S_{pp'}(-)$, is antisymmetric consistent with the above noted symmetry of γ_f and so of ψ_f in $\mathbf{R}_p$, $\mathbf{R}_{p'}$. The neutron spin wave function, $S_{nn'}(\pm)$ must be antisymmetric $(-)$ if the symmetric $(+)$ combination in $\mathbf{R}_n$, $\mathbf{R}_{n'}$ of the space wave functions γ_f is used, and vice versa.

Application of the conservation of total spin angular momentum now indicates that there are only four nonzero matrix elements of the type of Eq. (4) with ψ_i, ψ_f given in Eqs. (5), (6). The first of these is characterized by $S_{\text{tot}}=0$; $S_{\text{tot}}^{(z)}=0$; ψ_i space-symmetric for interchange of $\mathbf{R}_n$ with $\mathbf{R}_{n'}$; and ψ_f space-symmetric for interchange of $\mathbf{R}_n$ with $\mathbf{R}_{n'}$. The other three are characterized by $S_{\text{tot}}=1$; $S_{\text{tot}}^{(z)}=1,\ 0,\ -1$; ψ_i space-antisymmetric for exchange of $\mathbf{R}_p$, $\mathbf{R}_n$ with $\mathbf{R}_{p'}$, $\mathbf{R}_{n'}$; and ψ_f space-antisymmetric for interchange of $\mathbf{R}_n$ with $\mathbf{R}_{n'}$. Including the contributions of all of these possibilities gives

$$d\sigma/d\Omega\propto\{|h_d|^2-\tfrac{1}{3}h_d{}^*h_{d'}-\tfrac{1}{3}h_dh_{d'}{}^*+|h_{d'}|^2\},\quad(7a)$$

which in the case of real h_d, $h_{d'}$, [Eqs. (9), (12), (13)] becomes

$$d\sigma/d\Omega\propto h_d{}^2-\tfrac{2}{3}h_dh_{d'}+h_{d'}{}^2.\quad(7b)$$

h_d is a spatial integral of the form:

$$h_d=\tfrac{1}{2}\int\bigg[\gamma_f{}^*(\mathbf{R}_{n'},\mathbf{R}_p,\mathbf{R}_{p'})\exp(-i\mathbf{k}_n\cdot\mathbf{R}_n)\times\exp\left(i\mathbf{k}_n\cdot\frac{\mathbf{R}_{n'}+\mathbf{R}_{p'}+\mathbf{R}_p}{3}\right)\bigg]\times U\bigg[\psi_d(\mathbf{R}_n-\mathbf{R}_p)\psi_d(\mathbf{R}_{n'}-\mathbf{R}_{p'})\times\exp\left(i\mathbf{k}_d\cdot\frac{\mathbf{R}_n+\mathbf{R}_p}{2}\right)\exp\left(-i\mathbf{k}_d\cdot\frac{\mathbf{R}_{n'}+\mathbf{R}_{p'}}{2}\right)\bigg],\quad(8)$$

and $h_{d'}$ has the same form with the primed and unprimed quantities interchanged. We may also mention that the coefficient of the $h_dh_{d'}$ "interference" term was taken as zero in the earlier work of Chagnon and Owen[9] but, in agreement with our Eq. (7b), has been reported as $-\frac{2}{3}$ in a recent "wave vector" treatment of stripping by Owen and Madansky.[12]

Choosing an effective interaction potential U in Eq. (8) either in the manner of Butler[5] or of Bhatia,[13] one can express these spatial integrals as

$$h_d=\Lambda G(K)f(kR_0),\quad(9a)$$

$$h_{d'}=\Lambda G(K')f(k'R_0).\quad(9b)$$

In Eqs. (9a), (9b), the factor $G(K)$, the "internal momentum function," represents the probability that the captured proton has the momentum $\mathbf{K}$ within the "incident" deuteron. $G(K')$ has the analogous meaning for the "target" deuteron. $f(kR_0)$ and $f(k'R_0)$, the "centrifugal barrier terms," represent the probability that a proton traveling with the momentum $\mathbf{k}$, $\mathbf{k}'$ is found at a distance R_0 from the center of the capturing deuteron. The Λ function describes the net capture probability and, as it is not angle dependent, can be factored from the h_d and h_d' terms. The momentum vectors $\mathbf{K}$, $\mathbf{k}$ are defined in terms of the momentum $\mathbf{k}_d$ of the incident deuteron and the momentum $\mathbf{k}_n$ of the outgoing neutron by

$$\mathbf{K}(\theta)=\mathbf{k}_n-\tfrac{1}{2}\mathbf{k}_d,\quad(10a)$$

$$\mathbf{k}(\theta)=\mathbf{k}_d-\tfrac{2}{3}\mathbf{k}_n,\quad(10b)$$

with the relation between the primed and unprimed quantities being consistent with the symmetry about $\theta=90°$:

$$\mathbf{K}'(\theta)=\mathbf{K}(\pi-\theta),\quad(11a)$$

$$\mathbf{k}'(\theta)=\mathbf{k}(\pi-\theta).\quad(11b)$$

The quantitative expressions for $G(K)$ and $f(kR_0)$ in h_d depend of course upon the exact form of U which

[12] G. E. Owen and L. Madansky, Am. J. Phys. **26**, 260 (1958).
[13] Bhatia, Huang, Huby, and Newns, Phil. Mag. **43**, 485 (1952).

is used. Following Butler,[5] we have

$$G(K)=\left(\frac{8\pi\alpha_d}{\alpha_d^2+K^2}\right), \tag{12a}$$

where

$$\alpha_d\equiv\left(\frac{m_n}{\hbar^2}E_d\right)^{\frac{1}{2}}; \tag{12b}$$

and since the proton is captured into an $l_p=0$ orbit in He^3,

$$f(kR_0)=(2k_nR_0+1)\left\{\frac{J_{\frac{1}{2}}(kR_0)}{\sqrt{(kR_0)}} +kR_0\left[\frac{J_{-\frac{1}{2}}(kR_0)}{\sqrt{(kR_0)}}-\frac{J_{\frac{3}{2}}(kR_0)}{\sqrt{(kR_0)}}\right]\right\}, \tag{13}$$

where the $J_l(kR_0)$ are the spherical Bessel functions. Figure 5 shows the data compared with this expression. The solid curve in Fig. 5 was obtained by normalizing the plot of Eq. (7b) [with h_d and $h_{d'}$ given by Eqs. (9a)–(12b)] to the data at 23.5° c.m., and adding an isotropic background of 2.2 mb/steradian to each point. The ordinates of Figs. 4 and 5 give the absolute cross section directly in mb/steradian calculated from the yield of deuterons scattered into the monitor counter.

In the angular distribution described by the Eqs. (7), (9a), (9b), (12a), (12b), (13) there is only one adjustable parameter, the "interaction radius" R_0. The freedom of choice of this radius allows one to simulate to some extent the various effects that have been neglected, such as the interaction of the outgoing neutron with the residual nucleus, the Coulomb interaction between the incident and the target deuteron, etc. The magnitude of the radius must still have some physical significance, however, and the large value of $R_0=7\times10^{-13}$ cm which is necessary to fit the observed data emphasizes again the spatially extended nature of the deuteron.[14] It should also be mentioned that the slope of the angular distribution between 0° and 30° is quite sensitive to the radius used; thus $R_0=6.5\times10^{-13}$ cm and $R_0=7.5\times10^{-13}$ cm give poor fits to the experimental data.

In the preceding calculations we have used a central-force, delta-function interaction potential and considered S-state internal wave functions for the initial deuterons and the final He^3 nucleus; as a result we have no mechanism to produce a polarization of the outgoing neutrons. There have been, however, several experimental measurements of the polarization of these neutrons and also of the polarization of the protons from the companion (d,p) reaction, and polarizations in the neighborhood of 10–20% have been found.[15–19] To predict such polarizations from a stripping approach, it would be necessary to examine more carefully the effects which have been neglected. Thus in the matrix element of Eq. (4), one would have to allow an admixture of D state in the deuteron and He^3 internal wave functions; in addition, the interaction potential, U, would have to be expanded to include spin-orbit force and tensor force terms.

However, from the success of the simple stripping theory in fitting this and other observed angular distributions, one feels that these additional effects are small and not important for the determination of the angular distribution. Measurements are now under way at this laboratory to determine the magnitude of the polarizations of the emitted neutrons at this deuteron energy (8.4 Mev).

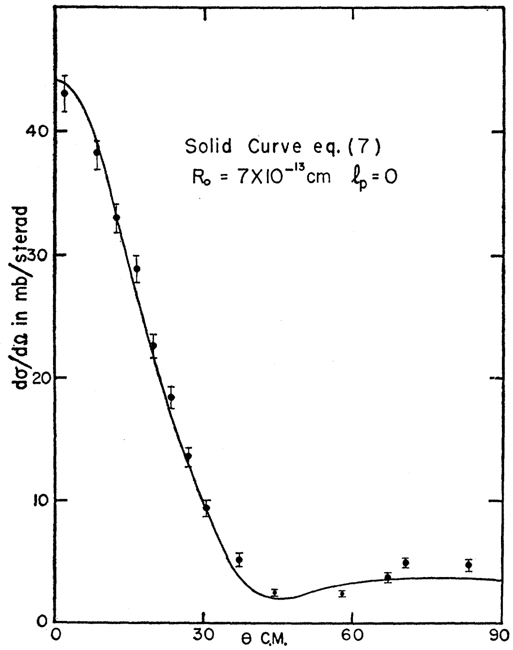

FIG. 5. Angular distribution of neutrons from $D(d,n)He^3$ at $E_d=8.4\pm0.1$ Mev fitted by nuclear stripping curve of Eq. (7) with $R_0=7\times10^{-13}$ cm and $l_p=0$.

ACKNOWLEDGMENTS

The authors wish to acknowledge stimulating discussion with Professor H. Primakoff and Dr. S. P. Rosen of Washington University, and Professor George Owen of the Johns Hopkins University, and also to acknowledge the assistance of Professor J. B. Reynolds and the entire cyclotron staff in the machine operation.

[14] The conventional "radius" of the deuteron is 4.3×10^{-13} cm. [J. M. Blatt and V. F. Weisskopf, *Theoretical Nuclear Physics* (John Wiley and Sons, Inc., New York, 1952), Chap. 2, p. 52.]

[15] McCormac, Steuer, Bond, and Hereford, Phys. Rev. **104**, 718 (1950).

[16] Meier, Scherrer, and Trumpy, Helv. Phys. Acta **27**, 577 (1954).

[17] Levintov, Miller, and Schamshev, Doklady Akad. Nauk S.S.S.R. **103**, 803 (1955).

[18] P. J. Pasma, Nuclear Phys. **6**, 141 (1958).

[19] R. J. Blin-Stoyle, Proc. Phys. Soc. (London) **A65**, 949 (1952); M. Fierz, Helv. Phys. Acta **25**, 629 (1952).